Proceedings of Global Power and Propulsion Society
ISSN-Nr: 2504-4400
GPPS Chania22
18th–20th September, 2022

www.gpps.global

GPPS-TC-2022-0091

DATA-DRIVEN MODELING OF HIGH-SPEED CENTRIFUGAL COMPRESSORS FOR AIRCRAFT ENVIRONMENTAL CONTROL SYSTEM

Andrea Giuffre'
Propulsion and Power
Faculty of Aerospace Engineering
Delft University of Technology
a.giuffre@tudelft.nl
Delft, The Netherlands, 2629HS

Federica Ascione
Propulsion and Power
Faculty of Aerospace Engineering
Delft University of Technology
f.ascione@tudelft.nl
Delft, The Netherlands, 2629HS

Carlo De Servi
Propulsion and Power
Faculty of Aerospace Engineering
Delft University of Technology
c.deservi@tudelft.nl
Delft, The Netherlands, 2629HS

Matteo Pini*
Propulsion and Power
Faculty of Aerospace Engineering
Delft University of Technology
m.pini@tudelft.nl
Delft, The Netherlands, 2629HS

ABSTRACT

The Environmental Control System (ECS) is the main consumer of non-propulsive power onboard aircraft, accounting for up to 3-5% of the total fuel consumption. The use of an electrically-driven Vapor Compression Cycle (VCC) system, in place of the conventional Air Cycle Machine (ACM), can lead to both a substantial increase of the Coefficient Of Performance (COP) at cruise conditions, and to a reduction of maintenance costs. The performance of the VCC system is highly affected by the design of its main components, namely, the compact heat exchangers and the high-speed centrifugal compressor. Therefore, the optimal system design requires the use of an integrated design methodology. This work documents the development of a data-driven compressor model based on Artificial Neural Networks (ANNs). The objective is to reduce the VCC model complexity, and the computational cost of the associated optimization problem. The model has been trained on a synthetic dataset composed of 165k unique centrifugal compressor designs generated with an in-house tool, validated with experimental data. The data-driven model has been coupled to an in-house integrated design framework for aircraft ECS, and it has been used to perform the multi-objective optimization of a VCC system for a single-aisle, short-haul aircraft, flying at cruise conditions. The results show that the number of function evaluations used to identify the Pareto front reduces by a factor of three, when leveraging the capabilities of the data-driven model. Moreover, the optimal solutions identified with the novel method cover a wider design space, due to the improved robustness of the VCC system model.

INTRODUCTION

The continuous improvement of aircraft fuel efficiency is, nowadays, a critical target in the aviation sector for economic, environmental and societal reasons. For this reason, the Advisory Council for Aeronautics Research in Europe (ACARE) is calling for innovative and sustainable technological solutions that can be adopted into the More Electric Aircraft (MEA). The goals set by Europe with the Flightpath 2050 call for a significant reduction of CO_2, NO_x, and noise emissions (ACARE, 2017). To reach these targets, a large number of resources have been invested in R&D programs for the development of new technologies for future aircraft, including investigation of alternative concepts for non-propulsive aircraft subsystems. Among all the auxiliary subsystems, the Environmental Control System (ECS) is the largest consumer of non-propulsive

*m.pini@tudelft.nl

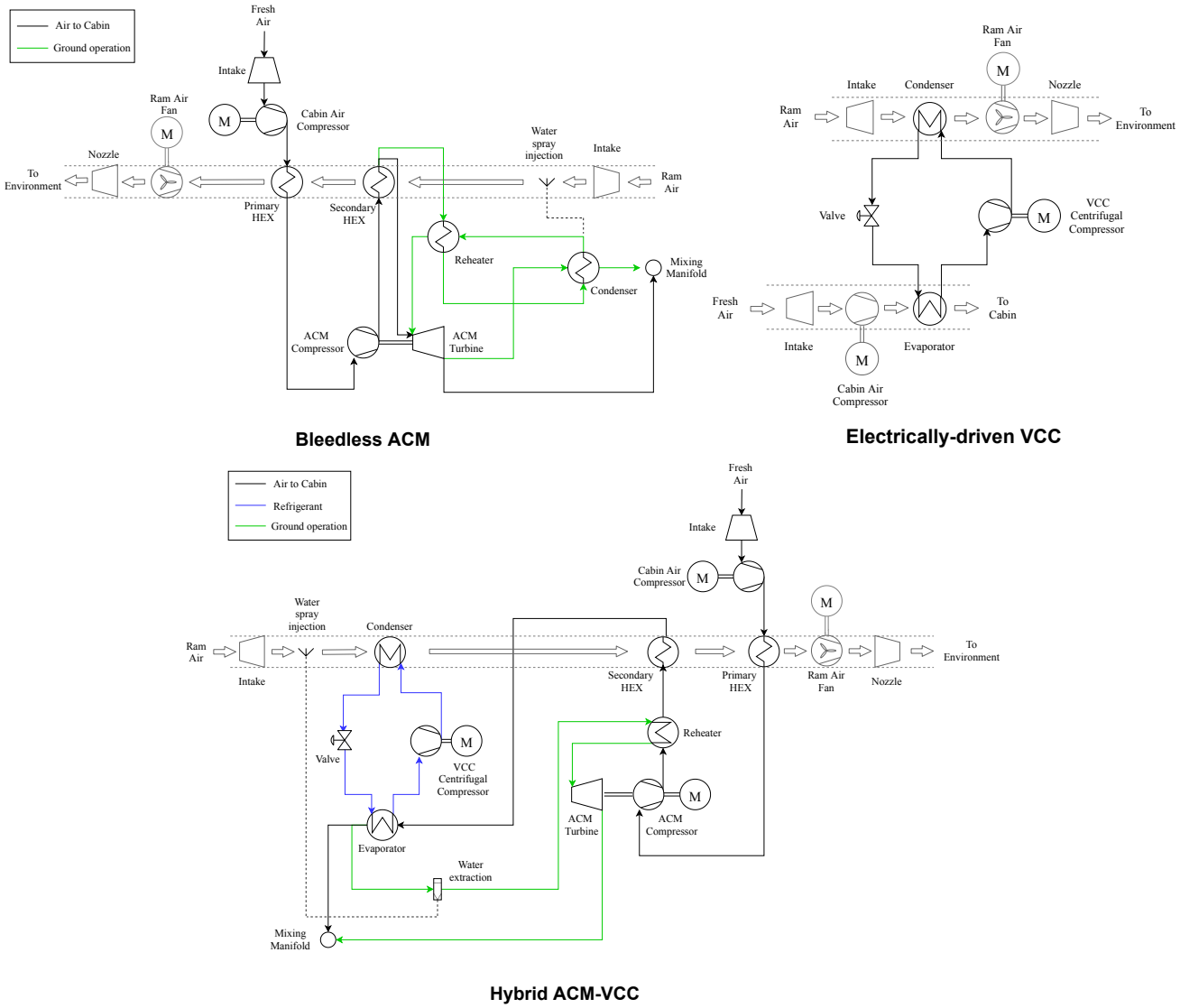

Figure 1 Simplified process flow diagram of three novel environmental control system architectures.

power, accounting for up to 3-5% of the total fuel burn (Bender, 2018). The ECS is responsible for providing dry, sterile and dust-free conditioned air to the airplane cabin at the proper temperature, flow rate and pressure, to satisfy the safety and comfort requirements, as well as to ensure adequate avionics cooling (Dechow and Nurcombe, 2005). To reduce the fuel consumption associated with the ECS, the Boeing 787 has been equipped with a bleedless ECS driven by an electrical motor, thus eliminating the need for pneumatic power generated by the engines. This solution enables a reduction of specific fuel consumption in the range of 1-2% at cruise conditions (Boeing, 2007). The replacement of the traditional Air Cycle Machine (ACM) with an electrically-driven Vapor Compression Cycle (VCC) system can lead to a substantial increase of the Coefficient Of Performance (COP) at cruise conditions. Moreover, the adoption of an electrically-powered ECS is expected to reduce maintenance costs and increase system reliability, due to the removal of the maintenance-intensive bleed system. On the other hand, the VCC system may not meet the high cooling power requirement, occurring under operating conditions such as ground operation at high ambient temperature and relative humidity. To overcome this limitation, Airbus and Liebherr are jointly developing a novel electrically-driven ECS concept based on a hybrid architecture, which integrates an ACM and a VCC system (Schmidt et al., 2021). A similar concept has been investigated also by DLR (Bender, 2018). Figure 1 shows the simplified process flow diagram of the three mentioned ECS architectures.
The performance of an electrically-driven VCC system is highly affected by the design of its main components, namely, the condenser, the evaporator, and the high-speed centrifugal compressor. Therefore, the maximization of the VCC system performance and its optimal design can be only achieved by resorting to an integrated design approach, i.e., a design framework in which the system is optimized together with its main components. Examples of application of such methodology for the design of conventional aircraft ECS can be found in Vargas and Bejan (2001); Pérez-Grande and Leo (2002). However, such studies lack a detailed modelling of the components; hence the optimization problem consists of a limited

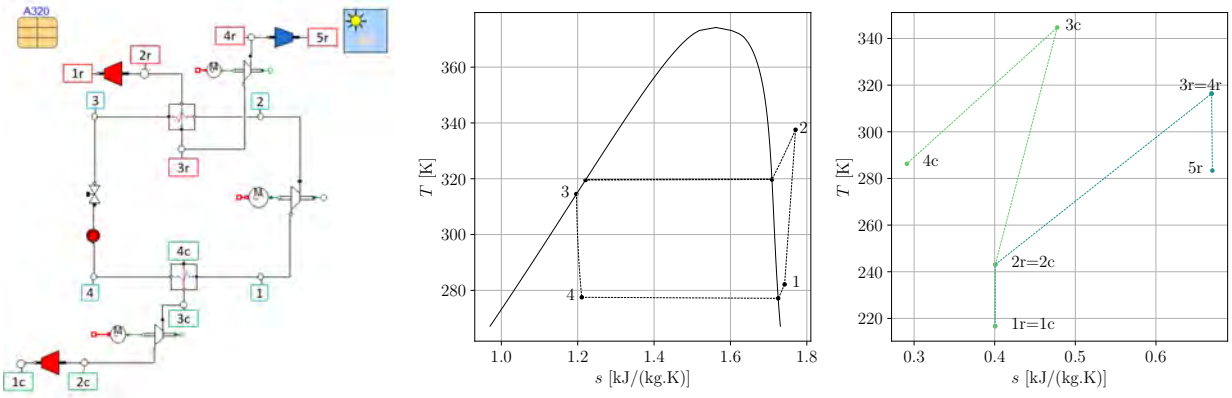

Figure 2 Modelica model of the electrically-driven VCC system. $T-s$ chart reproducing the thermodynamic processes occurring in the refrigeration loop (left chart), and in the ram and cabin air ducts (right chart).

number of design variables, and it does not account for any realistic constraint. As a consequence, the resulting configurations may be sub-optimal for the actual ECS. Moreover, no trade-off between system model complexity and computational cost has been addressed in these studies.

The objective of the present study is twofold: first, to propose a methodology to derive a data-driven model for high-speed centrifugal compressors, such as those of VCC systems; second, to demonstrate the capabilities of an optimization methodology exploiting this data-driven model for the integrated design of novel VCC-based ECS architectures. The paper is structured as follows. First, the models of the main components of the ECS are introduced, highlighting the main sources of complexity for system simulations. Then, the integrated design methodology is described and the problem of computational cost is discussed. Next, the data-driven compressor model is developed and coupled to the optimization framework to reduce the computational overhead associated to the compressor model, while retaining engineering accuracy. A multi-objective design optimization of the electrically-powered ECS is performed at cruise conditions with two different methodologies: a conventional one, where the compressor preliminary design is addressed by means of a mean-line code, and the proposed one, in which the meanline code is replaced with the data-driven compressor model. The results are compared in terms of optimal solutions and computational cost. Moreover, a sensitivity analysis is performed on five optimal designs selected over the Pareto front computed by means of the methodology adopting the data-driven compressor model. The purpose is to assess the robustness of the optimal solutions to changes in the values of the design variables, and to identify the design variables which mostly affect the objective functions. Finally, concluding remarks summarize the lessons learnt and provide an outlook for future work.

METHODOLOGY

The present work deals with the multi-objective optimization of an ECS for a single-aisle, short-haul aircraft, e.g., the Airbus A320. For the purpose of demonstrating the design methodology, only one ECS architecture and one operating condition are considered: a single-pressure level, electrically-driven VCC system, see Fig. 1, operating at cruise.

ELECTRICALLY-DRIVEN VCC FOR AIRCRAFT

The main components of the selected VCC system are two compact heat exchangers (CHEXs), namely the evaporator and the condenser, an expansion valve, and a high-speed centrifugal compressor operating on gas bearings. The use of a turbo-compressor, in place of a conventional scroll compressor, enables an increase of the system COP, while reducing its volume and weight. The COP of the VCC system can be further enhanced by adopting a configuration featuring multiple pressure levels. However, this is beyond the scope of the present work.

The VCC system has been modeled by resorting to the acasual (Schweiger et al., 2019), object-oriented, equation-based Modelica language. All the components are steady-state, zero-dimensional, and can be used for both design and off-design system simulations. The refrigerant selected for the application is the R-134a, i.e., a standard fluid for air conditioning systems. Figure 2 shows the in-house Modelica model of the electrically-driven VCC system, and illustrates the thermodynamic processes characterizing the system in the $T-s$ plane.

The evaporator and the condenser have the same topology, namely a bundle of flat tubes with an internal microchannel structure, and louver fins on the external surface. The fins and tubes geometries have been modeled following the guidelines provided in Shah and Sekulić (2003). The air and the refrigerant flow into the fins and the flat-tubes, respectively, according to an unmixed cross-flow arrangement. The refrigerant undergoes a phase change along the CHEXs tubes. To capture this phenomenon, the model of the device has been divided into a number of control volumes equal to the number of phases undertaken by the refrigerant during the thermodynamic process. For instance, the condenser is divided into

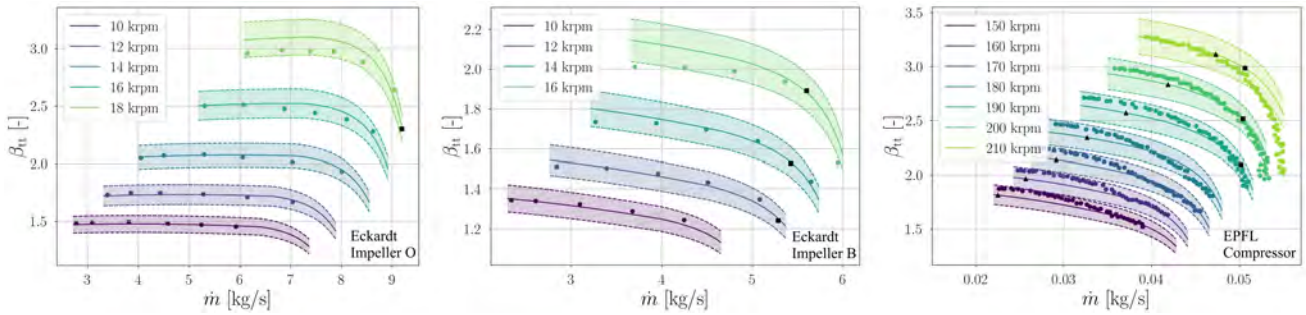

Figure 3 Validation of the in-house compressor model with experimental data. Solid lines represent compressor model predictions; dashed lines bound colored $\pm 5\%$ uncertainty bands; dots correspond to experimental data of Eckardt impellers O and B Eckardt (1977); Japikse (1987), and EPFL compressor Schiffmann and Favrat (2010). The estimated choking and rotating stall operating points are marked by ■ and ▲, respectively.

three sections: desuperheating (superheated vapour), condensation (two-phase flow) and subcooling (liquid phase). This modelling approach, known as Moving Boundary (MB) method, has been preferred to the Finite Volume (FV) method, since it guarantees a better trade-off between model complexity and accuracy, as demonstrated by Pangborn et al. (2015). By adopting the MB method, it is possible to estimate the heat transfer coefficient and the pressure drop in the CHEX using the most suitable correlations for each refrigerant phase. The set of correlations used in this study is reported in Ascione et al. (2021). Non-dimensional numbers, such as Colburn factor j, and friction factor f, are used to estimate the heat transfer coefficient and the pressure drop, respectively. Finally, the heat transfer rate is estimated using the ε-NTU method (Shah and Sekulić, 2003). The numerical models have been validated against the experimental results obtained by Kim and Bullard (2022).

The meanline model of the high-speed centrifugal compressor is an adaptation of the in-house tool documented in Giuffre' et al. (2022). The main simplifications with respect to the original model are: i) the use of a pure meanline approach, neglecting the radial evolution of flow quantities at the impeller inlet section, and along the vaneless diffuser; ii) the estimation of compressor performance only at design point. The compressor sizing is performed given ten design variables, namely: the swallowing capacity (ϕ_{t1}), the isentropic loading coefficient (ψ_{is}), the impeller shape factor (k), the total-to-total compression ratio (β_{tt}), the mass flow rate ($\dot{m}$), the impeller outlet absolute flow angle (α_2), the number of blades (N_{bl}), the diffuser radius ratio (R_3/R_2), and the non-dimensional parameters characterizing the shape of the diffuser ($R_{r,pinch}$, $H_{r,pinch}$). Moreover, the design of a compressor stage requires the specification of the working fluid, the total inlet conditions, and a list of geometrical parameters related to manufacturing constraints, e.g., the impeller tip clearance gap. The set of semi-empirical correlations proposed by Oh et al. (1997) has been implemented to estimate the impeller internal and external losses. Slip at the impeller outlet section is accounted for by means of the model derived by von Backström (2006). The vaneless diffuser losses are computed according to the method described in Amirante et al. (2015). Finally, the axial thrust acting on gas bearings is computed following the approach devised by Tiainen et al. (2021). Despite the simplifications, when integrated in the model of the VCC system, the compressor model significantly increases the non-linearity and complexity of the system of equations, and thus its solution, as well as the number of design variables. This leads to a substantial increment of computational cost when performing an integrated system design optimization.

DATA-DRIVEN COMPRESSOR MODEL

To reduce the complexity of the ECS model and the computational cost of the corresponding optimization problem, a data-driven compressor model has been developed and integrated into the existing framework. Several techniques are suitable for data-driven regression, e.g., symbolic regression, Artificial Neural Networks (ANN), Support Vector Machines (SVM), Gaussian Processes (GP). In the present work, a Multi-Layer Perceptron (MLP), i.e., a feedforward ANN featuring one or multiple fully connected hidden layers, has been selected to test the feasibility and evaluate the performance of the new integrated design optimization framework. Alternative methods for reduced-order modelling will be evaluated in a future work. Due to the lack of extensive open-source experimental data for high-speed centrifugal compressors, the MLP has been trained with synthetic data generated with the in-house compressor model documented in Giuffre' et al. (2022). The model has been validated with experimental data of reference impellers available in the open literature, as shown in Fig. 3. The synthetic dataset comprises 240k unique compressor stage designs, characterized by different combinations of the design variables listed in Tab. 1. The latin hypercube sampling method has been chosen to discretize the design space, defined by the ranges selected for each design variable. The additional compressor design parameters related to manufacturing constraints have been fixed to constant values, namely, $\varepsilon_b = \varepsilon_t = 0.15$ mm, $Ra = 3.2$ µm. Finally, in order to cope with the design of compressors of different size, the ratio among the shaft and the inlet hub

Table 1 Design space selected to create the database used to train the data-driven compressor model.

Variable	Range	Fluid	N	T_r	P_r
β_{tt}	2.0 - 5.0	H_2	3.0	2.0	0.08
$\dot{m}$ [kg/s]	0.05 - 0.25	CO_2	7.0	0.9	0.2
ϕ_{t1}	0.05 - 0.2	Propane	19.08	0.65	0.015
ψ_{is}	0.6 - 1.2	R-134a	21.64	0.65 - 0.81	0.015 - 0.15
α_2 [°]	60 - 75	Isobutane	28.43	0.65	0.015
k	0.65 - 0.95	R-1233zd(E)	28.77	0.65 - 0.82	0.015 - 0.15
N_{bl}	10 - 20				
R_3/R_2	1.2 - 2.0				
$H_{r,pinch} = \frac{H_3 - H_2}{H_2(R_2/R_{pinch} - 1)}$	0.0 - 1.0				
$R_{r,pinch} = \frac{R_{pinch} - R_2}{R_3 - R_2}$	0.0 - 1.0				

radii has been fixed throughout the design space, instead of prescribing a constant value of shaft radius.
The working fluids considered in the present study are synthetic and natural refrigerants selected from a parametric study conducted for an electrically-driven VCC for the ECS of large helicopters (Ascione et al., 2021). To enrich the dataset, the compressor stages operating with the refrigerants R-134a and R-1233zd(E) have been designed for two different total inlet thermodynamic states, resembling the conditions encountered in a conventional and a high-temperature heat pump. To reduce bias in the dataset and extend the range of applicability of the data-driven compressor model, the database has been complemented with compressor stages designed for simpler molecule fluids, i.e., CO_2 and H_2. Additional working fluids and thermodynamic conditions will be included as part of a future work. The complete list of fluids and reduced inlet conditions, i.e., total inlet conditions normalized with respect to critical state properties, considered in this work is reported in Tab. 1. To reduce the number of input features used to train the ANN and to avoid the use of categorical input, i.e., a string identifying the name of the fluid, the data associated to the working fluid and the inlet thermodynamic conditions have been synthesized in two parameters. These are the fluid molecular complexity, measured as the number of active degrees of freedom of a molecule (Colonna and Guardone, 2006)

$$N = \frac{2Mc_{v,id}(T_c)}{R}, \tag{1}$$

and the average value of the isentropic pressure-volume exponent (Kouremenos and Kakatsios, 1985) over the compression process

$$\overline{\gamma_{Pv}} = \frac{ln\left(\frac{P_{in}}{P_{out}}\right)}{ln\left(\frac{\rho_{in}}{\rho_{out}}\right)}. \tag{2}$$

A detailed analysis about the influence of these parameters on the design of centrifugal compressors can be found in Giuffre' et al. (2022), and it is omitted here for brevity. The resulting vector of input features for the ANN reads

$$X = \left[\phi_{t1},\ \psi_{is},\ \alpha_2,\ \frac{R_3}{R_2},\ k,\ N_{bl},\ H_{r,pinch},\ R_{r,pinch},\ \beta_{tt,target},\ \dot{m},\ N,\ \overline{\gamma_{Pv}},\ \frac{\varepsilon_b}{H_2},\ \frac{\varepsilon_t}{H_2}\right]. \tag{3}$$

The original dataset has been pre-processed by removing the compressor designs that are considered unfeasible, or do not meet the required specifications. The criteria used to filter the dataset are: minimum acceptable efficiency at design point $\eta_{tt} \geq 0.5$, minimum acceptable operating range at the design rotational speed $OR = \left.\frac{\dot{m}_{max} - \dot{m}_{min}}{\dot{m}_{des}}\right|_{\Omega_{des}} \geq 0.05$, maximum allowable blade angle at impeller outlet to ensure stable compressor operation $\beta_{2,bl} \leq 0°$, maximum allowable deviation between the target and the computed values of compression ratio $\Delta\beta_{tt} \leq 20\%$. The filtered dataset is composed by 165k samples, thus reducing the computational cost associated to the training of the data-driven model by about 30%, without any loss of useful information. In order to enhance the accuracy of the MLP model, input features standardization has been applied prior to training. Moreover, to further simplify the multivariate regression function to be learnt by the ANN,

Table 2 Design space and set of optimal hyperparameters.

Hyperparameter	Range	MLP_{obj}	MLP_{con}
L	4 - 6	5	6
$n^{[1]}$	5 - 200	199	60
$n^{[2]}$	5 - 200	199	94
$n^{[3]}$	5 - 200	200	44
$n^{[4]}$	5 - 200	144	63
$n^{[5]}$	5 - 200	42	68
$n^{[6]}$	5 - 200	-	70
α	10^{-4} - 10^{-1}	$10^{-2.75}$	$10^{-2.89}$
mini-batch size	2^6 - 2^{10}	2^6	2^6

Table 3 Accuracy of the two MLP models evaluated on the test set.

Y	$\text{mae} = \frac{1}{n}\sum_{i=1}^{n} \lvert \hat{Y} - Y \rvert$	$\text{mape} = \frac{1}{n}\sum_{i=1}^{n} \frac{\lvert \hat{Y} - Y \rvert}{Y} \cdot 100$
β_{tt}	0.031 [-]	0.96 %
η_{tt}	0.007 [-]	0.97 %
OR	0.013 [-]	4.97 %
$\dot{m}_{\text{choke}}$	0.004 [kg/s]	2.41 %
Ω_{des}	1670 [rpm]	1.01 %
$R_{1,\text{h}}$	10^{-5} [m]	0.31 %
H_2	10^{-5} [m]	0.84 %
$\beta_{2,\text{bl}}$	0.02 [deg]	0.37 %
R_4	$7 \cdot 10^{-4}$ [m]	1.06 %

the labels have been categorized according to their use in the ECS optimization process, i.e., objectives or constraints. Then, two separate MLP models have been trained to predict the vector of objective functions and constraints, namely:

$$\begin{aligned} Y_{\text{obj}} &= [\beta_{\text{tt}},\ \eta_{\text{tt}},\ OR,\ \dot{m}_{\text{choke}}], \\ Y_{\text{con}} &= [\Omega_{\text{des}},\ R_{1,\text{h}},\ H_2,\ \beta_{2,\text{bl}},\ R_4]. \end{aligned} \tag{4}$$

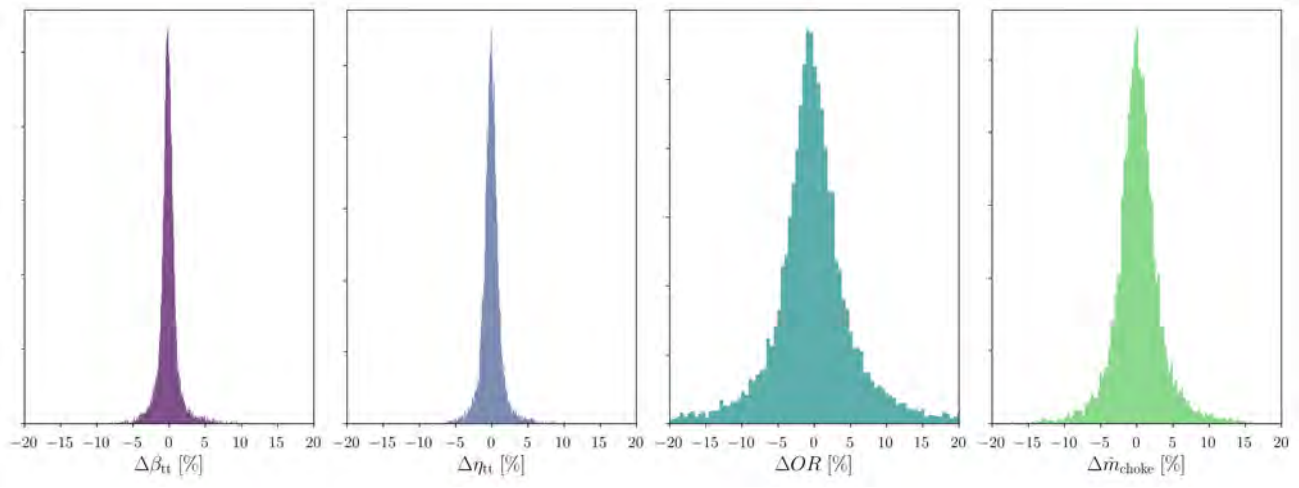

Figure 4 Distribution of the percentage error between the MLP model predictions and the true labels of Y_{obj}, evaluated on the test set.

Upon pre-processing, the dataset has been split into training, development, and test sets, counting 145k, 10k, and 10k samples, respectively. The space of hyperparameters investigated to optimize the accuracy of the ANN is summarized in Tab. 2. The hyperparameters search is performed by resorting to the NOMAD algorithm (Audet et al., 2019, 2021), i.e., an optimization algorithm suited for mixed-integer non-linear programming problems, featuring an expensive black-box function evaluation. For each combination of hyperparameters, a MLP model is created leveraging an open-source programming framework (Abadi et al., 2016), it is trained for 80 epochs, and its performance is evaluated on the development set, using the mean squared error loss function

$$L(\boldsymbol{\theta}) = \frac{1}{n}\sum_{i=1}^{n}(\hat{y}_i - y_i)^2, \tag{5}$$

where $\boldsymbol{\theta}$, n, and $\hat{y}$ denote the space of the hyperparameters, the number of samples, and the model prediction, respectively. The optimal architecture is selected after a maximum of 750 different MLP models have been trained and evaluated, and

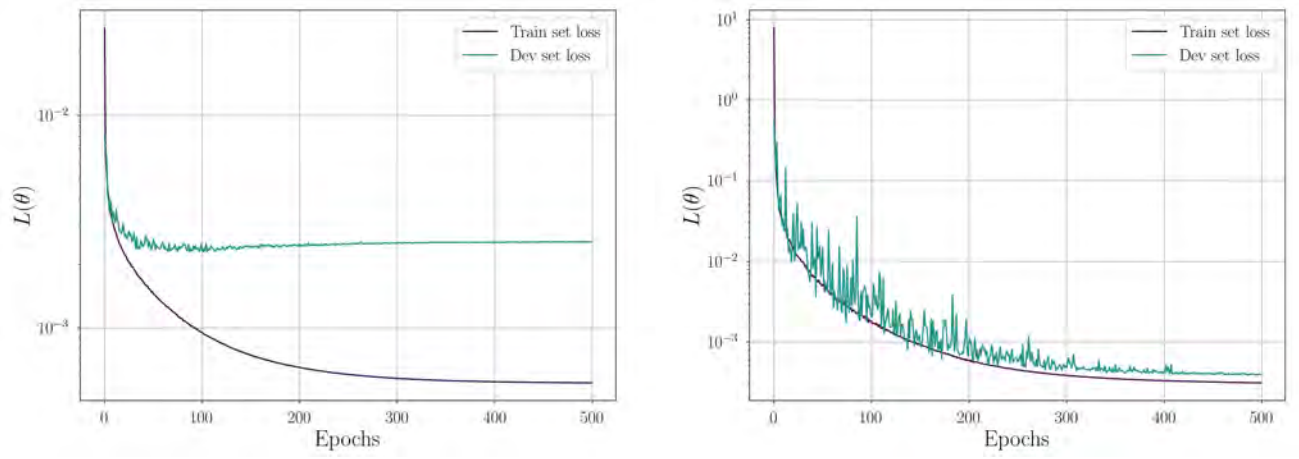

Figure 5 Training history of the MLP models trained to predict Y_{obj} (left) and Y_{con} (right), and featuring the optimal set of hyperparameters.

the process is repeated for both the models trained to predict Y_{obj} and Y_{con}. The arrays of optimal hyperparameters are reported in Tab. 2 for the two MLP models. The accuracy of the optimal MLP models is evaluated for each label on the test set, i.e., the 10k samples not used for training or hyperparameters search, in terms of both mean absolute error (mae), and mean absolute percentage error (mape). The results are listed in Tab. 3. Furthermore, to provide a more comprehensive overview of the predictive capabilities of the selected MLP models, the distribution of the percentage error evaluated on the test set is reported in Fig. 4 for the labels corresponding to the compressor objective functions, namely for each quantity of Y_{obj}. The same comparison has been performed for the labels corresponding to the compressor constraints Y_{con}, but it is omitted here for brevity. Eventually, the training histories of the MLP models featuring the optimal set of hyperparameters are displayed in Fig. 5.

ECS DESIGN OPTIMIZATION FRAMEWORK

The optimization of an aircraft ECS is a multi-disciplinary problem involving aspects related, but not limited, to: system performance, weight, installation, maintenance, safety, and life-cycle costs. For the sake of simplicity, the present study addresses an optimization problem involving three conflicting objectives, namely the maximization of the system COP, and the minimization of the weight and the drag penalty associated with its main components. With the purpose of evaluating the overall performance of the ECS, the COP is defined as the ratio of the power required for cabin cooling and pressurization in ideal conditions, over the total electric power consumption of the system, due to the cabin air compressor, the ram air fan and the high-speed centrifugal compressor:

$$\text{COP} = \frac{\dot{Q}_{\text{cooling}} + \dot{W}_{\text{p,id}}}{\dot{W}_{\text{el,CAC}} + \dot{W}_{\text{el,fan}} + \dot{W}_{\text{el,CC}}}. \tag{6}$$

To further simplify the problem, only the weight of the two CHEXs is accounted for as objective in the optimization process. The weight of the remaining components of the ECS is assumed to be constant. Due to the low operating temperature of the prescribed application, the material selected for both the condenser and the evaporator is the Aluminium alloy 6061. The weight minimization leads to CHEXs designs characterized by a high heat transfer surface to volume ratio. This design approach is beneficial in terms of heat transfer efficiency, but it often leads to higher pressure drops. To compensate for this effect, the third objective function selected in the present study addresses the minimization of the ram air drag. In mathematical form, the multi-objective optimization problem can be formulated as follows:

$$\begin{aligned}
&\min_{\boldsymbol{\alpha}\in\mathbb{R}^n} F(\boldsymbol{\alpha}) = [f_1(\boldsymbol{\alpha}),\ldots,f_{\text{n}_{\text{obj}}}(\boldsymbol{\alpha})], \quad \text{s.t.} \\
&h_k(\boldsymbol{\alpha}) = 0 \quad k = 1,\ldots,\text{n}_{\text{eq}} \\
&g_i(\boldsymbol{\alpha}) \leq 0 \quad i = 1,\ldots,\text{n}_{\text{ineq}} \\
&\alpha_{l,j} \leq \alpha_j \leq \alpha_{u,j} \quad j = 1,\ldots,\text{n}
\end{aligned} \tag{7}$$

where $\boldsymbol{\alpha}$ is the vector of design variables, $F(\boldsymbol{\alpha})$ is the vector of the objective functions, and $h_k(\boldsymbol{\alpha})$, $g_i(\boldsymbol{\alpha})$ are the vectors of the equality and inequality constraints, respectively. The non-linear constraints are imposed to ensure manufacturabil-

Table 4 Settings of the multi-objective optimization problem.

Design variable	Type	Range	Constraint	Value
$\dot{m}_{\text{ram}}$ [kg/s]	System	0.4 - 1.0	$\min(R_{1,\text{h}})$ [mm]	3.25
$\dot{m}_{\text{refr}}$ [kg/s]	System	0.1 - 0.25	$\min(H_2)$ [mm]	1.5
β_{tt}	System	2.0 - 5.0	$\min(\beta_{2,\text{bl}})$ [°]	-45
ΔT_{sh} [K]	System	3.0 - 10.0	$\max(\beta_{2,\text{bl}})$ [°]	-10
ΔT_{sc} [K]	System	3.0 - 10.0	$\max(\Omega)$ [krpm]	250
ϕ_{t1}	Compressor	0.05 - 0.2	$\min(x)\big\vert_{\text{eva-cond}}$ [mm]	50
ψ_{is}	Compressor	0.6 - 1.0	$\max(x)\big\vert_{\text{eva-cond}}$ [mm]	800
α_2 [°]	Compressor	60 - 75	$\min(\Delta T_{\text{pp}})\big\vert_{\text{eva}}$ [K]	3
k	Compressor	0.65-0.95	$\min(\Delta T_{\text{pp}})\big\vert_{\text{cond}}$ [K]	5
N_{bl}	Compressor	10 - 20	$\max(V_{\text{air}})\big\vert_{\text{eva-cond}}$ [m/s]	30
R_3/R_2	Compressor	1.2 - 2.0	$\max(V_{\text{refr}})\big\vert_{\text{eva-cond}}$ [m/s]	30
$R_{\text{r,pinch}}$	Compressor	0.0 - 1.0		
$H_{\text{r,pinch}}$	Compressor	0.0 - 1.0		
$y\big\vert_{\text{eva-cond}}$ [mm]	Heat exchanger	100 - 300		
$z\big\vert_{\text{eva}}$ [mm]	Heat exchanger	20 - 70		
$z\big\vert_{\text{cond}}$ [mm]	Heat exchanger	10 - 60		

ity of the system components, i.e., heat exchangers and compressor, and to define an upper threshold for the speed of the air and the refrigerant in the circuit. Overall, the optimization problem comprises 17 design variables, 3 objectives and 15 inequality constraints, as summarized in Tab. 4.

The in-house optimization framework consists of a Python program coupling the ECS model developed in Modelica with an open-source toolbox for multi-objective design optimization (Blank and Deb, 2020). The Pareto front of optimal solutions is computed by means of the NSGA-II algorithm described in Deb et al. (2002). The initial population comprises ten individuals for each design variable, and is sampled according to the latin hypercube methodology along the floating-point directions, and randomly along the integer axis, i.e., the one corresponding to the number of compressor blades. The population is evolved for a maximum of 170 generations, leading to a maximum of 28900 evaluations of the Modelica model. The result thereof is that the computational cost quickly becomes prohibitive when increasing the number of design variables, even if resorting to parallel computing to evaluate the individuals of each generation.

To overcome this limitation, the integrated design framework has been modified by replacing the compressor model implemented in Modelica with the pre-trained MLP models described in the previous section. The computational cost of the optimization problem can be significantly reduced by limiting the number of design variables selected by the stochastic algorithm NSGA-II. This can be achieved by resorting to the pre-trained MLP models, as described in the following.

The vector of design variables $\boldsymbol{\alpha}$ can be conveniently split into three subsets, corresponding to the design variables of the system, the heat exchangers, and the high-speed compressor:

$$\begin{aligned}
\boldsymbol{\alpha}_{\text{sys}} &= [\dot{m}_{\text{ram}},\ \dot{m}_{\text{refr}},\ \beta_{\text{tt}},\ \Delta T_{\text{sh}},\ \Delta T_{\text{sc}}], \\
\boldsymbol{\alpha}_{\text{HEX}} &= [y\big\vert_{\text{eva}},\ y\big\vert_{\text{cond}},\ z\big\vert_{\text{eva}},\ z\big\vert_{\text{cond}}], \\
\boldsymbol{\alpha}_{\text{c}} &= [\phi_{\text{t1}},\ \psi_{\text{is}},\ \alpha_2,\ k,\ N_{\text{bl}},\ R_3/R_2,\ R_{\text{r,pinch}},\ H_{\text{r,pinch}}].
\end{aligned} \tag{8}$$

The vector of input features for the data-driven model can be assembled by combining $\boldsymbol{\alpha}_{\text{c}}$ with two variables in $\boldsymbol{\alpha}_{\text{sys}}$, namely, $\dot{m}_{\text{refr}}$, β_{tt}, and with two parameters related to compressor manufacturability, i.e., $\varepsilon_{\text{b}}/H_2$, $\varepsilon_{\text{t}}/H_2$, and two parameters related to the prescribed working fluid and thermodynamic state, i.e., N, $\overline{\gamma_{Pv}}$. In turn, the set of compressor design variables $\boldsymbol{\alpha}_{\text{c}}$ can be decoupled from the array of optimization variables selected by the stochastic algorithm, and can be treated separately. In the present implementation, once the values of β_{tt} and $\dot{m}_{\text{refr}}$ have been selected by the stochastic algorithm for each individual of a generation, the set of $\boldsymbol{\alpha}_{\text{c}}$ is optimized separately, by resorting to a constrained gradient-based algorithm (Kraft, 1988). The values of the objectives and constraints are evaluated by means of the MLP models, and the objective function is expressed as a linear combination of η_{tt} and OR. After the gradient-based optimization, the resulting values of η_{tt} and β_{tt} are appended to the vectors $\boldsymbol{\alpha}_{\text{sys}}$ and $\boldsymbol{\alpha}_{\text{HEX}}$, and the values of objectives and constraints of the VCC system are computed by means of the Modelica model. Eventually, the compressor operating range can be in-

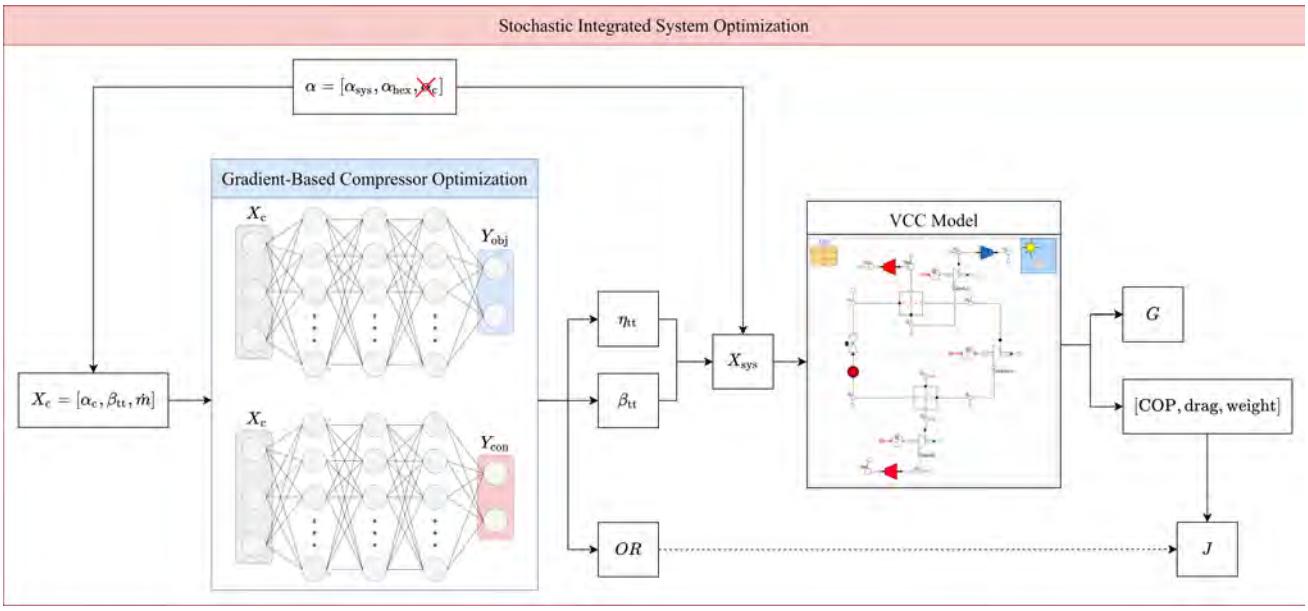

Figure 6 Flowchart of the modified ECS optimization framework. The data-driven model is used to decouple the optimization of the high-speed centrifugal compressor, highlighted in blue, from the optimization of the VCC system, highlighted in red.

cluded into the vector of objective functions J. However, this is not done in the present work, since the aim is to compare the Pareto front identified by means of the original and the modified ECS optimization framework, without altering the vector of the objective functions. The modified optimization methodology is schematically illustrated in Fig. 6.
Thanks to the use of data-driven modeling, the cost of the compressor optimization for each individual of the population is negligible, as compared to the cost associated with the evaluation of the VCC system model. On the other hand, the number of design variables selected by the stochastic algorithm drops from 17 to 9, leading to a sizeable reduction of the number of objective function evaluations needed to reach convergence.

RESULTS AND DISCUSSION

The test case selected to benchmark the performance of the original and the modified integrated design framework is the multi-objective optimization of an electrically-driven VCC system for the ECS of a single-aisle, short-haul aircraft, e.g., the Airbus A320. The aircraft is assumed to fly at cruise conditions, namely at $M_\infty = 0.78$, and at an altitude of 11.88 km. The environmental conditions are computed according to the International Standard Atmosphere (ISA) model. The working fluid selected for the VCC system is the refrigerant R-134a. The inlet conditions of the mixing manifold of the air distribution system, which corresponds to the outlet of the VCC system, are specified in terms of mass flow rate, pressure, and temperature: $\dot{m}_{mix} = 0.5\,kg/s$, $P_{mix} = 76.25\,kPa$, $T_{mix} = 13.14\,°C$. The water content in the air at cruise altitude is negligible, thus the effect of humidity is disregarded. As mentioned above, the objectives selected for the optimization study are: the system COP, the weight of the CHEXs, and the drag penalty associated to the ECS. The design variables and the non-linear constraints are listed in Tab. 4.
The multi-objective optimization performed with the original framework, namely the one adopting the system model with the compressor meanline code, reached convergence after a total of 13050 function evaluations. On the other hand, the number of function evaluations reduces to 4500 when resorting to the modified optimization framework, leveraging the data-driven compressor model. This enables a reduction of the total computational time from approximately 125 hours to 37.5 hours, when running the optimization in parallel on an Intel® Xeon® E5-1620 v3 CPU, featuring eight logical threads.
The Pareto front computed with the modified optimization framework is displayed in Fig. 7. The COP of the entire ECS, see Eqn. (6), is reported on the x-axis of the left figure, whereas the COP of the VCC system, i.e., the ratio between the cabin cooling duty ($\dot{Q}_{cooling}$) and the electrical power required by the centrifugal compressor ($\dot{W}_{el,CC}$), is reported on the x-axis of the right figure. The same results are illustrated on the weight-drag, COP-weight, and COP-drag planes in Fig. 8, and they are compared with the ones computed with the original optimization framework.
The main outcomes can be summarized as follows. As expected, the minimization of the CHEXs weight and the maximization of the COP are conflicting objectives. In the same fashion, the minimization of the CHEXs weight and of the drag penalty are in trade-off. The use of very compact and lightweight heat exchangers leads to larger pressure drops, thus higher drag penalty, and to smaller heat transfer surfaces, thus heat exchange under larger temperature gradients. Nevertheless, the optimization results show that it is possible to achieve a compact and lightweight design of the heat ex-

changers, without incurring in large drag penalty. However, the attainment of such heat exchanger designs comes at the expense of a reduction in the COP of the system.

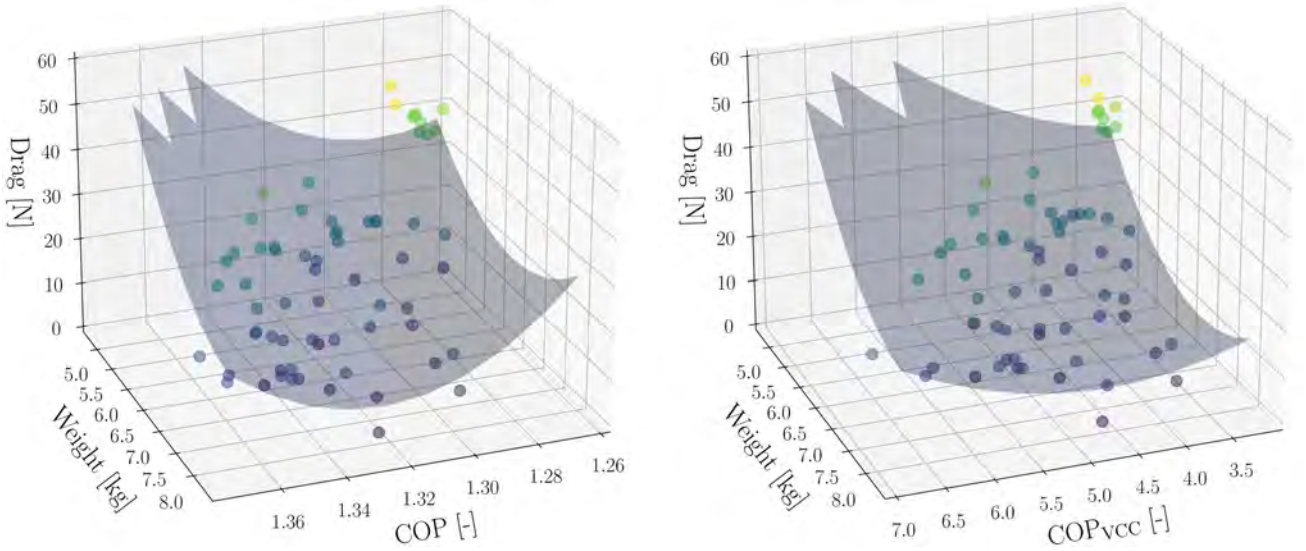

Figure 7 Pareto front computed with the modified optimization framework coupled to the data-driven compressor model, considering the COP of the entire ECS (left), and the COP of the VCC system (right).

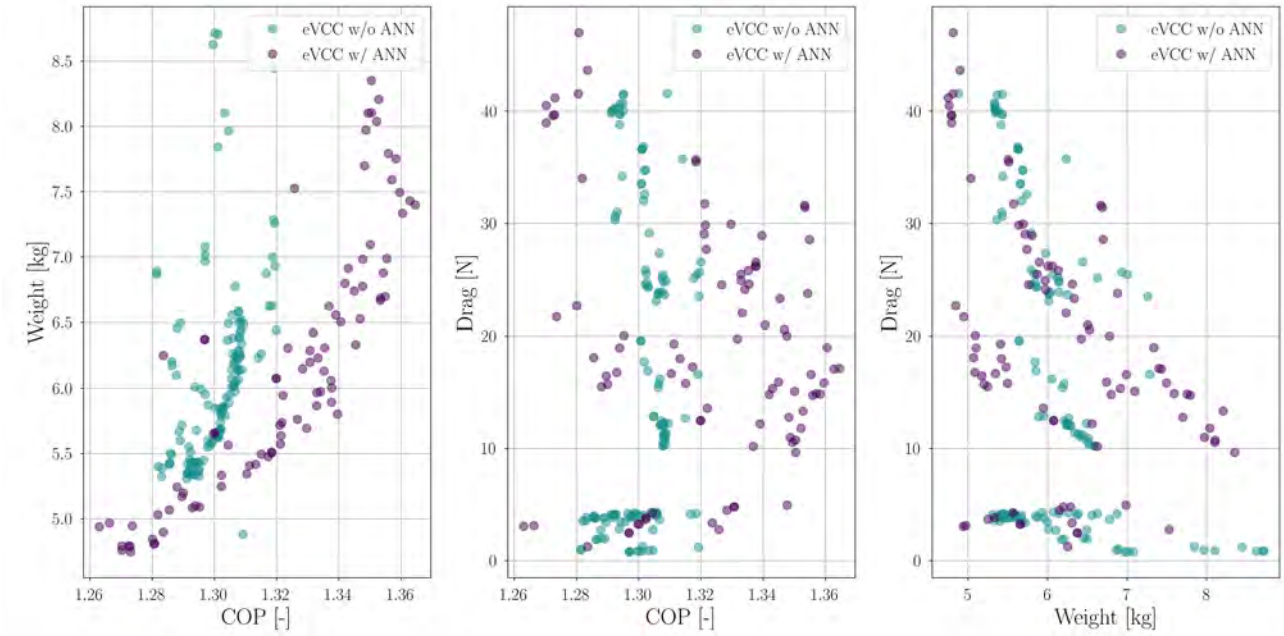

Figure 8 Comparison between the trends established among the objective functions, computed with and without the use of the data-driven compressor model, coupled to the integrated design optimization framework.

Furthermore, by comparing the optimal design points identified with the original and the modified integrated design methodology, it is possible to observe that: i) similar trends are established among the three objectives; ii) the range of variation of weight and drag penalty over the Pareto front is comparable; iii) the design methodology exploiting the data-driven compressor model is able to identify optimal solutions characterized by higher COP. To provide a physical explanation of the difference in the COP computed with the two methods, it is possible to refer to Fig. 9, showing the trend of the mechanical power required by the refrigerant compressor as a function of the COP of the ECS, and of the VCC system. Since the cabin cooling requirement is fixed in the study, the COP of the system is inversely proportional to the power required by the refrigerant compressor, hence to the compression ratio β_{tt}. The use of the data-driven compressor model leads to optimal design solutions featuring a wider range of β_{tt}, thus a wider range of COP values. The root cause

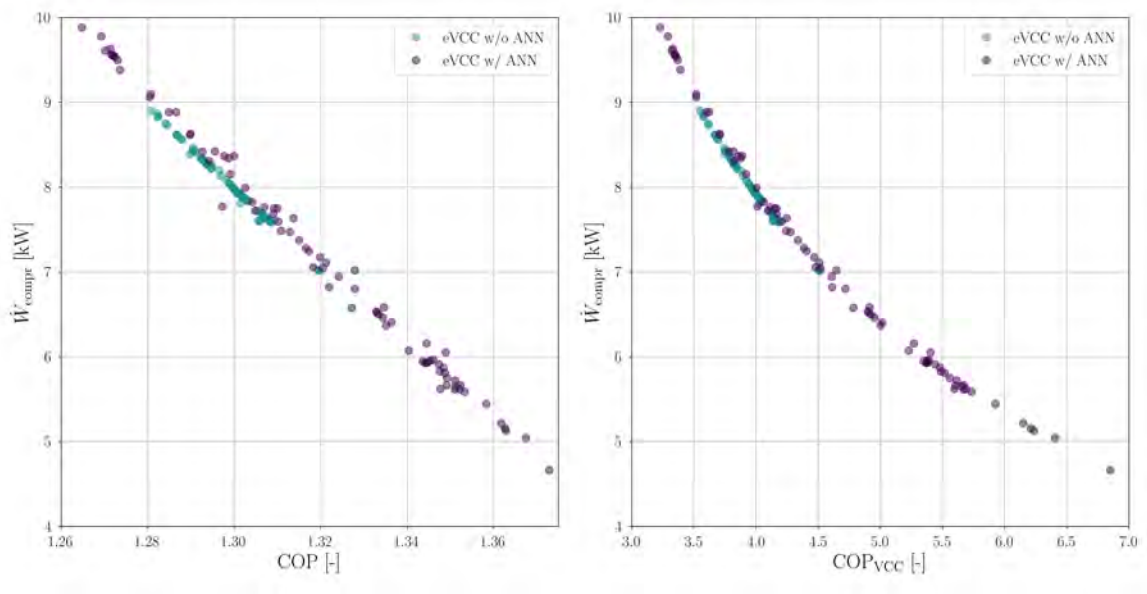

Figure 9 Comparison between the trends of the refrigerant compressor mechanical power vs. the COP of the ECS (left), and of the VCC system (right), computed with and without the use of the data-driven compressor model.

of this difference can be arguably attributed to the higher complexity of the VCC system model integrating the compressor meanline code, which makes the solution of the underlying non-linear system of equations more susceptible to failure during the optimization process.

A sensitivity analysis of the objective functions with respect to the prescribed set of design variables is finally performed. The purpose is to assess the robustness of the solutions with respect to changes in the values of the design variables, as well as to identify those variables which mostly affect the objective functions. The analysis is carried out as follows. First, five design points are selected over the Pareto front computed with the modified optimization framework. Then, a perturbation of $\pm 10\%$ is applied to each design variable independently, and the vector of objective functions is re-evaluated. This process is repeated for each prescribed design point, and the averaged results are displayed in Fig. 10. The sensitivity of the objective functions is evaluated with respect to the compressor efficiency η_{tt}, rather than to the compressor design variables $\boldsymbol{\alpha}_c$. Moreover, for the present investigation, the COP of the ECS is replaced with the COP of the VCC system since the former is mainly affected by the terms $\dot{W}_{p,id}$ and $\dot{W}_{el,CAC}$ in Eqn. (6), whose values are almost constant in the simulations.

The outcomes of the sensitivity analysis can be summarized as follows. The COP shows the highest sensitivity with respect to the mass flow rate of refrigerant, and to the pressure ratio and the efficiency of the refrigerant compressor. The weight of the CHEXs is mostly affected by the mass flow rates of refrigerant and ram air. The value of drag penalty shows the highest sensitivity with respect to $\dot{m}_{refr}$, $\dot{m}_{ram}$, z_{cond}, y_{eva}, and β_{tt}. As a result, the computational cost of the optimization process can be further reduced by removing z_{eva}, y_{cond}, ΔT_{sh}, and ΔT_{sc} from the vector of design variables, without significantly affecting the optimal solutions. Moreover, the COP of the optimal designs shows a variation of the order of $\pm 10\%$, when changing the values of the compressor efficiency and the refrigerant mass flow rate by $\pm 10\%$. These results highlight that the COP of the VCC system is relatively insensitive to, e.g., variations in the thermodynamic cycle parameters and to the performance of the components, except for the compressor. On the other hand, the weight and the drag penalty of the optimal system designs are significantly more affected by changes in the design variables, in particular, the mass flow rate of refrigerant and ram air.

CONCLUSIONS

The capabilities offered by an integrated design framework for aircraft ECS embedding a data-driven model for high-speed compressor preliminary design have been investigated in this work. The reduced-order model has been trained on synthetic data generated by a validated in-house compressor model, and it has been used in combination with an in-house design framework for aircraft ECS to perform the multi-objective optimization of an electrically-driven VCC system for a single-aisle, short-haul aircraft, flying at cruise. The main outcomes of this study can be summarized as follows.

1. A data-driven compressor model can be developed using a database of about 165k compressor designs. The number of design variables considered to create the dataset of compressor stage designs is relatively limited, thanks to the adoption of a non-dimensional approach based on scaling analysis. To enhance the accuracy of the data-driven

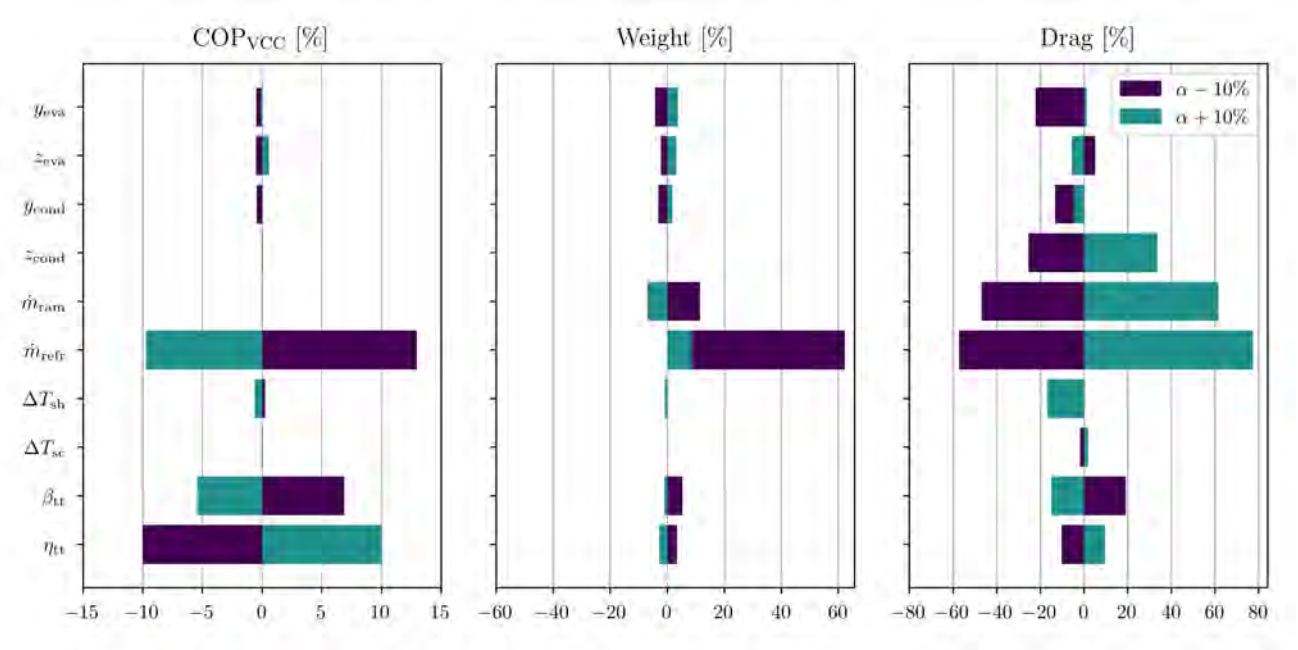

Figure 10 Sensitivity of the objective functions with respect to a $\pm 10\%$ perturbation in the vector of design variables. The analysis is repeated for five optimal design points selected over the Pareto front identified with the modified optimization framework, and the results are averaged.

compressor model, and to facilitate its integration in the ECS optimization framework, two MLP models have been trained to predict the compressor performance parameters and the relevant geometrical constraints. The mean absolute percentage error of the two MLP models evaluated on the test set is 2.32% and 0.72%, respectively.

2. The complexity of the VCC system model, and the likelihood of an ill-conditioned matrix when the associated mathematical problem is solved, can be reduced by replacing the high-speed centrifugal compressor with a data-driven model. A similar approach could be adopted to replace also the models of the condenser and the evaporator.

3. The use of data-driven models enables the partial decoupling between the optimization of the VCC system and of the high-speed compressor. For each set of system design variables selected by the stochastic algorithm, the compressor design variables are optimized by resorting to a constrained gradient-based algorithm. As a result, the number of design variables selected by the stochastic algorithm drops from 17 to 9.

4. The number of expensive function evaluations needed to identify the Pareto front reduces from 13050 to 4500, if the integrated design framework is properly modified to leverage the capabilities of the data-driven model. On the other hand, the range of variation of the objective functions and the trends established among them remain virtually unaltered, regardless of the adopted compressor model. Moreover, the modified framework is able to identify optimal solutions in a wider design space, thanks to the improved robustness of the underlying VCC system model.

5. As pointed out by a sensitivity analysis, the computational cost of the optimization process can be further reduced by removing z_{eva}, y_{cond}, ΔT_{sh}, and ΔT_{sc} from the vector of design variables, without significantly affecting the solution. Furthermore, the COP of the VCC system is less sensitive than the weight and the drag penalty to variations in the values of the thermodynamic cycle parameters and components performance, except for the compressor efficiency.

The results of this research reveal the large potential of adopting data-driven models for the simultaneous optimization of a thermodynamic process and the preliminary design of its components. The substantial reduction of the computational cost associated to the optimization process, combined with the improved robustness of the underlying system model, make this approach suitable for large-scale, industrial-strength design applications, and pave the way for further investigation of non-conventional ECS architectures.

ACKNOWLEDGMENTS

The authors gratefully acknowledge the student Fridolin Haugg for contributing to the initial development of the data-driven compressor model. This research was supported by the Dutch Technology Foundation TTW, Applied Science Division of NWO, the Technology Program of the Ministry of Economic Affairs, and by Aeronamic BV (Grant No. 17091).

NOMENCLATURE

Acronyms

ACM	Air Cycle Machine
ANN	Artificial Neural Network
CHEX	Compact Heat Exchanger
CO_2	Carbon Dioxide
COP	Coefficient Of Performance
ECS	Environmental Control System
FV	Finite Volume
H_2	Hydrogen
mae	Mean absolute error
mape	Mean absolute percentage error
MB	Moving Boundary
MLP	Multi-Layer Perceptron
NTU	Number of Thermal Units
R-1233zd(E)	Trifluoropropene
R-134a	Tetrafluoroethane
VCC	Vapour Compression Cycle

Greek Symbols

α	Absolute flow angle	[deg]
β	Compression ratio	[−]
$\boldsymbol{\alpha}$	Vector of design variables	[−]
$\boldsymbol{\theta}$	Vector of hyperparameters	[−]
ε	Effectiveness	[−]
ε_b	Back face clearance	[mm]
ε_t	Tip clearance gap	[mm]
η	Efficiency	[−]
γ_{Pv}	Isentropic pressure-volume exponent	[−]
ν	Poisson's ratio	[−]
Ω	Rotational speed	[rpm]
Φ_{t1}	Swallowing capacity	[−]
ψ_{is}	Isentropic loading coefficient	[−]
ρ	Density	[kg/m^3]
k	Impeller shape factor	[−]

Subscripts

1	Impeller inlet
2	Impeller outlet
3	Diffuser outlet
4	Volute outlet
CC	Cabin Compressor
con	Constraints
el	Electrical
h	Hub
is	Isentropic
obj	Objectives
pp	Pinch point
sc	Subcooling
sh	Superheating
ts	Total-to-static
tt	Total-to-total

Non Dimensional Numbers

Ma	Mach number
Re	Reynolds number

Roman Symbols

$\dot{m}$	Mass flow rate	[kg/s]
$\dot{Q}$	Heat flow rate	[W]
$\dot{V}$	Volumetric flow rate	[m^3/s]
$\dot{W}$	Power	[W]
$\hat{Y}$	Vector of model predictions	[−]
D	Diameter	[m]
f	Friction factor	[−]
F_{ax}	Axial thrust	[N]
H	Blade height	[m]
h	Specific enthalpy	[J/kg]
j	Colburn factor	[−]
k	Impeller shape factor	[−]
L	Loss function	[−]
N	Fluid molecular complexity	[−]
n	Number of samples	[−]
N_{bl}	Number of blades	
OR	Operating range	[−]
P	Pressure	[Pa]
R	Radius	[m]
Ra	Surface roughness	[μm]
T	Temperature	[K]
t	Thickness	[mm]
U	Peripheral speed	[m/s]
V	Absolute velocity	[m/s]
W	Relative velocity	[m/s]
Y	Vector of true labels	[−]

REFERENCES

Abadi, M., Barham, P., Chen, J., Chen, Z., Davis, A., Dean, J., Devin, M., Ghemawat, S., Irving, G., Isard, M., Kudlur, M., Levenberg, J., Monga, R., Moore, S., Murray, D. G., Steiner, B., Tucker, P., Vasudevan, V., Warden, P., Wicke, M., Yu, Y. and Zheng, X. (2016), TensorFlow: A system for Large-Scale machine learning, *in* '12th USENIX Symposium on Operating Systems Design and Implementation (OSDI 16)', USENIX Association, Savannah, GA, pp. 265–283.

ACARE (2017), Strategic Research and Innovation Agenda, Technical report, Advisory Council for Aviation Research and Innovation in Europe.

Amirante, R., De Bellis, F., Distaso, E. and Tamburrano, P. (2015), 'An Explicit, Non-Iterative, Single Equation Formulation for an Accurate One Dimensional Estimation of Vaneless Radial Diffusers in Turbomachines', *Journal of Mechanics* **31**(2), 113–122.

Ascione, F., De Servi, C. M., Meijer, O., Pommé, V. and Colonna, P. (2021), Assessment of an Inverse Organic Rankine Cycle System for the ECS of a Large Rotorcraft Adopting a High-Speed Centrifugal Compressor and a Low GWP Refrigerant, *in* '6 th International Seminar on ORC Power Systems'.

Audet, C., Le Digabel, S., Rochon Montplaisir, V. and Tribes, C. (2021), NOMAD version 4: Nonlinear optimization with the MADS algorithm, Technical report, Les cahiers du GERAD.

Audet, C., Le Digabel, S. and Tribes, C. (2019), 'The Mesh Adaptive Direct Search Algorithm for Granular and Discrete Variables', *SIAM Journal on Optimization* **29**(2), 1164–1189.

Bender, D. (2018), Exergy-based analysis of aircraft environmental control systems and its integration into model-based design, PhD thesis, Berlin.

Blank, J. and Deb, K. (2020), 'Pymoo: Multi-Objective Optimization in Python', *IEEE Access* **8**, 89497–89509.

Boeing (2007), AERO, 4th quarter, Technical report.

Colonna, P. and Guardone, A. (2006), 'Molecular interpretation of nonclassical gas dynamics of dense vapors under the van der Waals model', *Physics of Fluids* **18**(5), 056101.

Deb, K., Pratap, A., Agarwal, S. and Meyarivan, T. (2002), 'A fast and elitist multiobjective genetic algorithm: NSGA-II', *IEEE Transactions on Evolutionary Computation* **6**(2), 182–197.

Dechow, M. and Nurcombe, C. (2005), *Aircraft Environmental Control Systems*, Springer Berlin Heidelberg, Berlin, Heidelberg, pp. 3–24.

Eckardt, D. (1977), Investigation of the jet-wake flow of a highly loaded centrifugal compressor impeller, PhD thesis, NASA Headquarters Washington, DC United States.

Giuffre', A., Colonna, P. and Pini, M. (2022), 'The effect of size and working fluid on the multi-objective design of high-speed centrifugal compressors', *International Journal of Refrigeration* .

Japikse, D. (1987), 'A critical evaluation of three centrifugal compressors with pedigree data sets: Part 5-studies in component performance', *Journal of Turbomachinery* **109**(1), 1–9.

Kim, M.-H. and Bullard, C. W. (2022), 'Performance Evaluation of a Window Room Air Conditioner With Microchannel Condensers', *Journal of Energy Resources Technology* **124(1): 47-55**, 9.

Kouremenos, D. A. and Kakatsios, X. K. (1985), 'The three isentropic exponents of dry steam', *Forschung im Ingenieurwesen* **51**(4), 117–122.

Kraft, D. (1988), A software package for sequential quadratic programming, Technical report, DLR German Aerospace Center – Institute for Flight Mechanics, Koln, Germany.

Oh, H. W., Yoon, E. S. and Chung, M. K. (1997), 'An optimum set of loss models for performance prediction of centrifugal compressors', *Proceedings of the Institution of Mechanical Engineers, Part A: Journal of Power and Energy* **211**(4), 331–338.

Pangborn, H., Alleyne, A. G. and Wu, N. (2015), 'A comparison between finite volume and switched moving boundary approaches for dynamic vapor compression system modeling', *International Journal of Refrigeration* **53**, 101–114.

Pérez-Grande, I. and Leo, T. J. (2002), 'Optimization of a commercial aircraft environmental control system', *Applied Thermal Engineering* **22**(17), 1885–1904.

Schiffmann, J. and Favrat, D. (2010), 'Design, experimental investigation and multi-objective optimization of a small-scale radial compressor for heat pump applications', *Energy* **35**(1), 436–450.

Schmidt, S. A., Riedel, J., Hepcke, F., Casas, W., Bonhora, J., Lavergne, D., Sanchez, F. and Ricard, G. (2021), New Air Systems for More Electric Aircraft, *in* 'More Electric Aircraft 2021'.

Schweiger, G., Nilsson, H., Schoeggl, J., Birk, W. and Posch, A. (2019), 'Modeling and simulation of large-scale Systems: a systematic comparison of modeling paradigms'.

Shah, R. K. and Sekulić, D. P. (2003), *Fundamentals of heat exchanger design*, John Wiley & Sons, Hoboken, NJ.

Tiainen, J., Jaatinen-Värri, A., Grönman, A., Sallinen, P., Honkatukia, J. and Hartikainen, T. (2021), 'Validation of the Axial Thrust Estimation Method for Radial Turbomachines', *International Journal of Rotating Machinery* **2021**, 1–18.

Vargas, J. V. and Bejan, A. (2001), 'Integrative thermodynamic optimization of the environmental control system of an aircraft', *International Journal of Heat and Mass Transfer* **44**(20), 3907–3917.

von Backström, T. W. (2006), 'A Unified Correlation for Slip Factor in Centrifugal Impellers', *Journal of Turbomachinery* **128**(1), 1–10.